Synthesis, Characterization and Biological studies of metal oxides and Silver doped metal oxides nanoparticles

P.Amutha[1], S.Gomuraj[2], A.Mathavan[3]

[1,2,3] PG & Research Department of Chemistry, V.O.Chidambaram College, Tuticorin-628 008, Tamilnadu, India.

Abstract- **Nanoparticles exhibit a number of interesting characteristics including unique physical, chemical, optical, magnetic and electrical properties. Vanadium pentoxide, cerium oxide, samarium Oxide, Ag doped vanadium pentoxide, Ag doped cerium oxide, Ag doped Samarium Oxide nanoparticles and V2O5-CeO2, V2O5-Sm2O3 nanocomposites are prepared by chemical methods. The prepared nanoparticles are characterized by using analytical techniques such as FT-IR, UV-visible, XRD, SEM, AFM and TEM analysis. The interaction of metal oxides with mixed and doped metal oxides nanoparticles are studied by UV-visible absorption spectroscopy studies. The stretching and bending vibrations of metal oxides doped metal oxides are characterised by using FT-IR techniques. The X-ray diffraction studies (XRD) have shown crystallite size of nanoparticles around 18 nm to 52 nm. The particle sizes and morphology of nanoparticles are determined through Scanning Electron Microscope (SEM), Transmission Electron Microscope (TEM) and Atomic force Microscope (AFM). The measured band gap energy values are in the range from 2.38 to 4.39 eV which indicates that all the nanomaterials are semiconductive in nature except cerium oxide. The Ag doped V2O5 nanoparticles are highly active towards antimicrobial activities.**

Keywords: Vanadium pentoxide, Samarium oxide, mixed metal oxides, doped metal oxides.

INTRODUCTION:

Metal oxide and mixed oxide nanoparticles (NPs) have great potential for electronic, magnetic, optical, and photocatalytic applications. Mixed oxide system composed of two or more different components has attracted particular interest because their unique properties are not usually attainable in single components. Metals highly dispersed on nanosupport surfaces show active catalysts for a variety of reactions [1]. The numerous methods have been documented in the recent reviews for the synthesis of a broad range of metal oxide and mixed oxide NPs [2]. Among them, sol-gel processes have fascinated many researchers in contemporary science owing to the advantages of simple process, easy scale-up and low cost. In fact, particle sizes, surface areas and mechanical properties of the materials obtained by these methods can be changed according to the temperature, operating conditions, and to the used precursor [3].

Nanoparticles have been utilised newly to develop the present imaging techniques for in vivo diagnosis of biomedical disorders [4].Presently, iron oxide nanoparticles are being used in patients for both diagnosis and therapy, leading to more effective medication with less unfavourable effects [5]. An exclusive, susceptible and greatly explicit immune assay system based on the aggregation of gold nanoparticles that are coated with protein antigens, in the attendance of their corresponding antibodies, was also developed [6]. Nanoparticles, as drug delivery systems, are capable to uplift the several crucial properties of free drugs, such as solubility, in vivostability, pharmacokinetics, biodistribution and enhancing their efficiency [7]. In this context, we discuss the synthesis, characterization and biological studies of metal oxides and silver doped metal oxides nanoparticles[8].

EXPERIMENTAL PROCEDURE

Preparation of nanoparticles

Preparation of vanadium pentoxide (V_2O_5) nanoparticles

The ammonium metavanadate (NH_4VO_3) was dissolved in hot distilled water and after the complete dissolution of ammonium metavanadate in which the NH_3 gas was removed by con. HNO_3 was added to the solution at 100°C. The resultant colour solution is red in nature and then abruptly changed to brown coloured precipitate. The resulting precipitate was collected by filtration, washed with water, and dried in a vacuum oven at 100°C for 24 hours. The precipitate was dispersed in ethanol with stirring, and the solvent was removed by evaporation. This process was repeated atleast 5 times with ethanol. The solvent-exchanged precipitate was collected by the filtration and was dried in a vacuum oven at 100°C for 24 hours. The yellow solid of V_2O_5 nanoparticles was obtained [9].

Preparation of samarium oxide (Sm_2O_3) nanoparticles

The calcination products of samarium nitrate hexahydrate, $Sm(NO_3)_3.6H_2O$ abbreviated as SmNit were obtained by heating at various temperatures (200-600ºC) for one hour in the presence of air. The calcination temperatures were chosen on the basis of the thermal analysis results. The calcination products were kept dry over silica gel to obtain yellowish white solid of Sm_2O_3 nanoparticles.SmNit600 which indicates the decomposition products of SmNit at 600ºC for one hour.

Preparation of cerium oxide (CeO_2) nanoparticles

Nanocrystalline cerium oxide particles are synthesized by the combustion of aqueous solutions containing ceric ammonium nitrate, citric acid and glycine. The aqueous solution is prepared by dissolving the stoichiometric amount of ceric ammonium nitrate (CAN), and glycine (G) and citric acid (CA) in water. The solution is agitated in a beaker using magnetic stirrer for 3hours. The resulting solution is kept in an electric furnace set at 200ºC, during which it evaporates foams and then undergoes flameless combustion resulting nanocrystalline oxide and the fine powder is very light and porous. The synthesised ceria powder are still impure as it contains the gases are not dissolved and which are removed by calcinations at 400ºC for 3 hours in a muffle furnace to obtain pale yellow solid of cerium oxide nanoparticle[10].

Preparation of mixed metal oxides nanocomposites

The mixed oxides materials were prepared by an acid-catalyzed sol-gel process and about 0.6g of vanadium pentoxide was dissolved in 40 ml of hydrogen peroxide[11]. The resulting solution was stirred for 30 min and then a mixture containing 0.4g of samarium oxide/cerium oxide, 3ml of acetic acid and 25ml of propanol-2 was added into solution while stirring. The green gel was obtained and dried at 80oC, then calcined at 300°C for 6 hours under an air flow to obtain dark green solid of nanocomposites[12].

Preparation of Ag doped V_2O_5 nanoparticles

The ammonium metavandate (NH_4VO_3) was dissolved in hot distilled water and after the complete dissolution of ammonium metavanadate the NH_3 gas was removed and then 1% of $AgNO_3$ solution and concentrated nitric acid were added to the solution at 100ºC. The resultant colour solution is red in nature and then abruptly changed to brown coloured precipitate. The resulting precipitate was collected by filtration, washed with water, and dried in a vacuum oven at 100ºC for 24 hr. For the solvent exchange, the precipitate was dispersed in organic solvent (ethanol) with stirring, and then the solvent was removed by evaporation[13]. This process was repeated atleast 5 times with ethanol. The solvent-exchanged precipitate was collected by the filtration and was dried in a vacuum oven at 100ºC for 24 hr to afford yellowish orange solid of Ag doped V_2O_5 nanoparticles[14].

Preparation of Ag doped CeO_2 nanoparticles

Nanocrystalline cerium oxide particles are synthesized by the combustion of aqueous solutions containing ceric ammonium nitrate and citric acid plus glycine. The aqueous solution is prepared by dissolving the stoichiometric amount of ceric ammonium nitrate (CAN), ((NH4)2Ce (NO3)6) and glycine (G) and citric acid (CA) in distilled water. Then 1% of AgNO3 solution was added. The solution is then agitated in a beaker using magnetic stirrer for 3h. The resulting solution is kept in an electric furnace set at 200ºC, during which it evaporates foams and then undergoes flameless combustion resulting nanocrystalline oxide. This fine powder is very light and porous. These as synthesised ceria powder are still impure as it contains the undissolved gases which are removed by calcinations at 400ºC for 3 hrs in a muffle furnace to afford black colour solid of Ag doped CeO2 nanoparticles[15].

RESULTS AND DISCUSSION

UV-visible absorption spectroscopy

The UV-visible absorption (DRS) spectra of nanoparticle, nanocomposites and Ag doped nanoparticles in solid phase measurement have been shown in Fig.1. In the case of mixed nanocomposites, the absorption band is found to have increases at 500 nm to 900 nm (isobestic point) than individual V2O5, CeO2 andSm2O3 nanoparticle .]This might be due to the change in the size of the particle in nano range and also colour changes to green colour. The absorption band for Ag doped nanoparticle is found to have less and more absorption than undoped nanoparticle. This might be due to the interaction between Ag ion and metal oxides lattice.

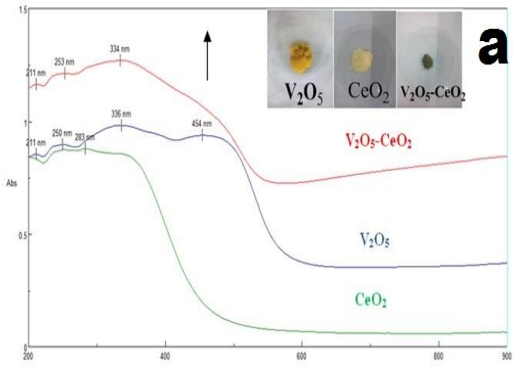

Fig.1 UV-visible absorption spectra of a) V_2O_5, CeO_2, V_2O_5-CeO_2

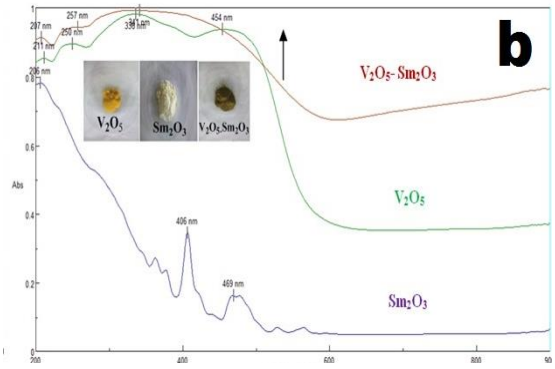

b) V_2O_5, Sm_2O_3, V_2O_5-Sm_2O_3

FT-IR analysis

The FT-IR spectrum used as a tool to determine the various metal oxide stretching and bending vibrations of nanoparticles [16]. The bands appearing in the range 400 to 1200 cm-1 were assigned to various stretching and bending vibrations of metal-oxide-metal stretching and bending vibrations. The sharp band at around 1000-1100 cm-1 indicates the presence of Metal-oxide stretching frequency. The band observed between at 3500-3300 cm-1 and 1650-1600 cm-1 were attributed to the absorptions of hydroxyl group from adsorbed water of metal oxides.

X-ray diffraction analysis

The XRD pattern of prepared nanoparticle, nano composites and Ag doped nanoparticles were recorded. The most important diffraction peaks are observed at 2θ values and the corresponding originating planes are indentified. The crystalline nature of nanoparticles is confirmed by observed sharp diffraction peaks from the XRD pattern and the XRD parameters. The XRD pattern of V2O5 nanoparticles is shown in the Fig.2. The average crystallite size of nanoparticle and nanocomposites were calculated by using Scherrer's equation.It clearly suggests that the diffraction peaks obtained for V2O5, CeO2, Sm2O3, V2O5-CeO2, Ag doped V2O5 and Ag doped CeO2 nanoparticle are very sharp indicating the crystalline nature of nanoparticles.

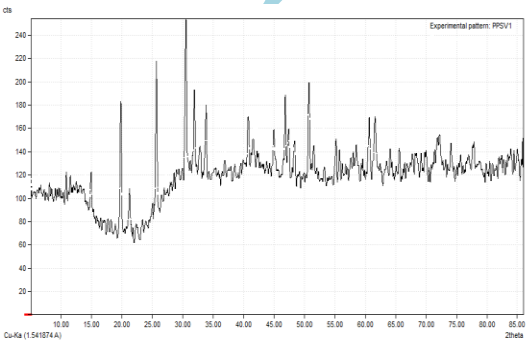

Fig. 2. XRD pattern of V_2O_5 nanoparticles

Determination of Band gap energy

The term "band gap" refers to the energy difference between the top of the valence band to the bottom of the conduction band. The electrons are able to jump from one band to another. In order for an electron to jump from a valence band to a conduction band, it requires a specific minimum amount of energy for the transition, the band gap energy. Measuring of the band gap is important in the semiconductor and nanomaterial industries [17].

The band gap energy in a nanomaterial could be obtained from the absorption maxima. According to quantum confinemental theory, electrons in the conduction band and holes in the valence band are spatially confined by the potential barrier of the surface. Due to confinement of both electrons and holes, the lowest energy optical transition from the valence band to the conduction band will increase in energy, effectively increasing the band gap (Eg). The shoulder or peak of the spectra corresponds to the fundamental absorption edges in the samples, and could be used to estimate the band gap of the nanomaterial[18].From the absorption peak the optical energy band gap of V_2O_5, Ag doped V_2O_5, CeO_2 and Ag doped CeO_2,V_2O_5- CeO_2,V_2O_5-Sm_2O_3 ,Sm_2O_3 and Ag doped Sm_2O_3 nanoparticles have been calculated using the formula,

$$E_g = h\nu_g = hc/\lambda_g$$

Where h = plank's constant and E_g= energy band gap of the semi conducting nanoparticles in the optical spectra. The band gap energy of nanoparticles is calculated and which is shown in Table 1. T he band gap energy of CeO_2 nanoparticles is higher than the other nanoparticles. We concluded that the size of CeO_2 nanoparticles is decreased. The band gap energy values are in the range from 2.38 to 4.39 eV which indicates that all the nanomaterials are semiconductive in nature except cerium oxide.

Table: 1 Band Gap energy values of V_2O_5, Ag doped V_2O_5, CeO_2 and Ag doped CeO_2, V_2O_5-CeO_2, V2O5-Sm_2O_3, Sm_2O_3 and Ag doped Sm_2O_3 nanoparticles.

S. No	Nanoparticles	λ(nm)	Band gap energy $E\times10^{19}$ (J)	Band gap energy (eV)
1	V_2O_5	454	4.38	2.74
		336	5.92	3.70
2	Ag doped V_2O_5	454	4.38	2.74
		380	5.23	3.27
3	V_2O_5- CeO_2	334	5.95	3.72
4	V_2O_5-Sm_2O_3	341	5.83	3.64
5	CeO_2	283	7.02	4.39
6	Ag doped CeO_2	521	3.82	2.38
7	Sm_2O_3	469	4.24	2.65

		406	4.90	3.06
8	Ag doped Sm_2O_3	522	3.81	2.38
		407	4.88	3.05

Scanning Electron Microscopy analysis

Morphology and structure of the samples were investigated by Scanning Electron Microscopy (SEM). Fig. shows that the surface morphology of V_2O_5 nanoparticles exhibits smoothy like structure whereas Ag doped V_2O_5 nanoparticles exhibits nanochips like structure. The surface morphology of CeO_2 nanoparticles shows fibre, sponge like structure whereas Ag doped CeO_2 nanoparticles reveals flake like structure. While Sm_2O_3 nanoparticles exhibits flake, flower like structure whereas in the case of Ag dopped Sm_2O_3 nanoparticles exhibits fibre, flower like structure. Also, it is clear that mixed nanocomposite reveals sponge like structure [19].SEM image of
V_2O_5 and Sm_2O_3 are shown in the figure 3.

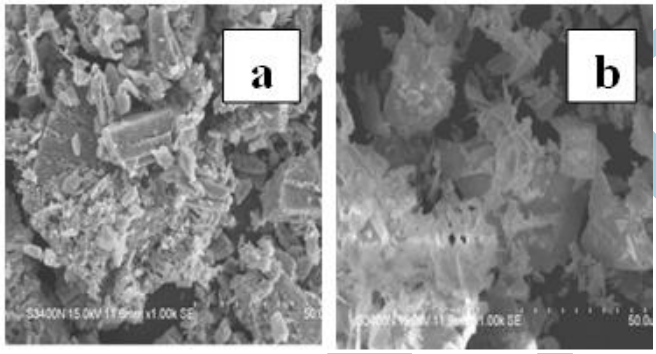

Fig.3 SEM image of V_2O_5 and Sm_2O_3

Energy Dispersive X-Ray Analysis

Energy dispersive X-Ray analysis was carried out to find out the elemental composition of the synthesized nanoparticles.EDX pattern of V_2O_5, Ag doped V_2O_5, CeO_2, Ag doped CeO_2, Sm_2O_3, Ag doped Sm_2O_3 is shown in the figure 4.

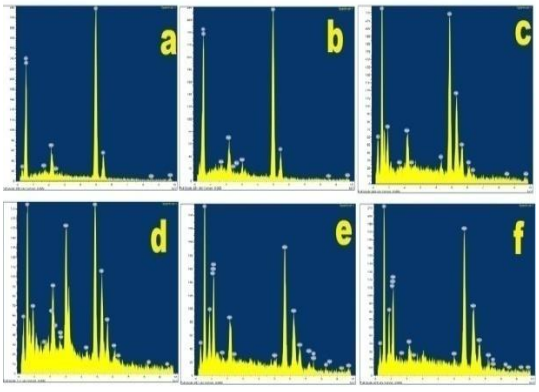

Fig.4 EDX pattern of a) V_2O_5, b) Ag doped V_2O_5, c) CeO_2, d) Ag doped CeO_2, e) Sm_2O_3, f) Ag doped Sm_2O_3 nanoparticles

Transmission Electron Microscopy analysis

From the TEM image, we found that the size of V_2O_5 nanoparticles size 21 nm exhibits sheet like structure and fibre in nature, otherwise called as nanofibre[20]. Also, it is clear that most of the Ag doped V_2O_5 nanoparticles are spherical in shape and its size 9.28 nm.While in the case of V_2O_5-CeO_2 nanocomposites size 4.01 nm which are spherical in shape whereas V_2O_5-Sm_2O_3 nanocomposite is unambiguously assigned from the TEM images that they are nanorod in shape and its size 35.28 nm. TEM image of V_2O_5 is shown in the figure 5.

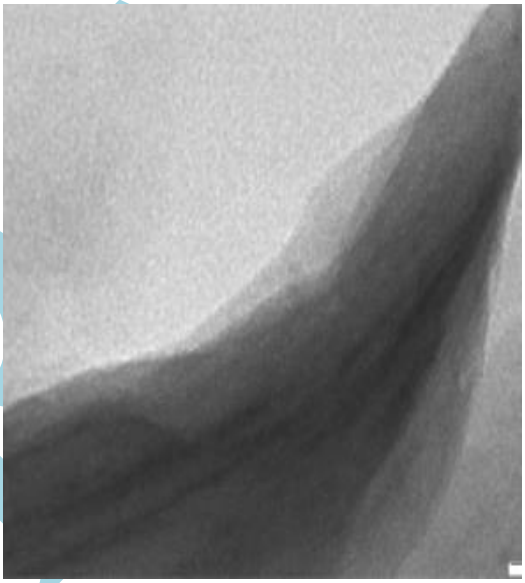

Fig.5 TEM image of V_2O_5

Biological study

Antibacterial activity

Invariably all the eight nanoparticles showed different antibacterial activity; inhibit growth of pathogen considerably. The antibacterial activity of zone of inhibition of nanoparticles. The maximum level of zone of inhibition (14 mm) was observed for Ag doped V_2O_5 nanoparticles (VA) against *Pseudomonous* which shows that it has high activity and CeO_2(C) and V_2O_5-Sm_2O_3(VS) nanoparticles has no activity with the bacterias like *Pseudomonas*, *Klebsiella*, *B.subtilis* and *Enterococcus.* The metal oxide nanoparticles like V_2O_5 (V) Ag doped V_2O_5(VA), Ag doped CeO_2(CA), Sm_2O_3(S), Ag doped Sm_2O_3 (SA) and V_2O_5-Sm_2O_3(VS) with the bacteria *Klebsiella*. Among all the nanoparticles the Ag doped V_2O_5 nanoparticles has more antibacterial activity than other nanoparticles. Thus form the zone of inhibition; it was evident that the synthesized nanoparticles have potent antibacterial activity[21]. The Antibacterial activity of Zone of inhibition levels are shown in Table: 2 and Antibacterial activity of *Klebsiella* are shown in figure 6.

Table: 2 Zone of inhibition of nanoparticles.

S. No	Bacteria	Zone of inhibition level (mm) at 500 µg/well						Control(Amikacin)
		V	VA	CA	S	SA	VC	VS
1	*Klebsiella*	8	11	9	8	8	10	31
2	*Pseudomonas*	10	14	10	–	–	9	16
3	*B.subtilis*	8	11	8	–	–	10	20
4	*Enterococcus*	–	10	7	–	–	–	9

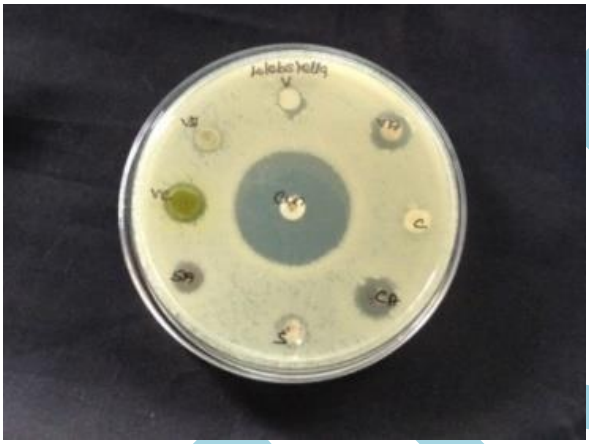

Fig.6 Antibacterial activity of nanomaterials by Klebsiella.

S. No	Fungus	Zone of inhibition level (mm) at 500 µg/well								Control (Fluconazole)
			VA	C	CA	S	SA	VC	VS	
1	*Aspergillusflaves*	–	10	–	7	–	–	–	–	–
2	*Aspergillusoryzae*	–	10	–	–	–	–	–	–	–
3	*Actinomyces*	–	9	–	–	–	–	–	–	–
4	*Talaromycesflaves*	–	11	–	7	10	8	12	15	–

Fig.7 Antifungal activity of nanomaterials by Aspergillusflaves.

Antifungal activity

Invariably all the eight nanoparticles showed different antifungal activity; inhibit growth of pathogen considerably. Antifungal activity of Zone of inhibition of nanoparticles is shown in Fig. 7.2. The maximum level of zone of inhibition (15 mm) was observed VS = V2O5-Sm2O3 nanoparticles against Talaromycesflaves. C= CeO2 nanoparticles did not inhibits the Aspergillusflaves, Aspergillusoryzae, Actinomyces and Talaromycesflaves. Talaromycesflaves fungus has more inhibition level of VA, CA, S, SA, VC, VS nanoparticles. VA= Ag doped V2O5 nanoparticles has more antifungal activity than other nanoparticles. Thus form the zone of inhibition; it was evident that the synthesized nanoparticles have potent antifungal activity [22]. The Antifungal activity of Zone of inhibition levels are shown in Table: 3 and Antifungal activity of Aspergillusflaves are shown in figure 7.

Table: 3 Zone of inhibition of nanoparticles.

CONCLUSION

Vanadium pentoxide, cerium oxide, Samarium Oxide, Ag doped vanadium pentoxide, Ag doped cerium oxide, Ag doped Samarium Oxide nanoparticles and V2O5-CeO2, V2O5-Sm2O3 nanocomposites were synthesized by chemical method. The nanoparticles were characterized using FTIR, UV-VIS, XRD, SEM, AFM and TEM. The surface morphology of the metal oxides nanoparticles is characterized by SEM as well as TEM analysis and suggested different morphological structures. The prepared compounds show good antimicrobial activity.

REFERENCES

1. Xia Y, Accounts of Chemical Research 46.8 2013, 1671-1672.

2. Mohammadi-Manesh, E.; Vaezzadeh, M.; Saeidi, M.,Surf. Sci. 2015, 636, 36-41.

3. Koziej, D.;Lauria, A.; Niederberger, Adv. Mater. 2014, 26, 235-257.

4. S A Hakim, Y Liu, G S Zakharova,RSC Advances, 52015 23489-23497.

5. Madkour LH. Advanced Nanotechnology3.1 2017: 15-18.

6. Abbasi E, Critical Reviews in Microbiology 42.2 2015: 170-180.

7. ParveenS, Nanoparticles and Nanomedicine 8.2 2012: 147-166.

8. Poulose.S, Journal of Nanosci and Nanotech 14.2 2014: 2038-2049.

9. T. Konya, T. Katou, T. Murayama, S. Ishikawa, M. Sadakane, D. Buttrey, W.Ueda, Catal. Sci. Technol. 3 2013 380.

10. Gönüllü, Y.; Haidry, A. A.; Saruhan, B. Sens. Actuators, B 2015, 217,78–87.

11. X H Yang, H T Fu, X Z An, X C Jiang, A B Yu,RSC Advances,62016 34103-34109.

12. Y-J Chen, G Xiao, T-S Wang, F Zhang, Y Ma, P Gao, C-L Zhu, E Zhang, Z Xu, Q- Li, Sens. and ActuatorsB: Chemical,1562011 867-874.

13. H Fu, X Yang, X Jiang, A Yu, Sens. and Actuators B: Chemical, 2032014 705-711.

14. H Fu, H Xie, X Yang, X An, X Jiang, A Yu,Nanoscale Research Lett., 10 2015 1-12.

15. Wang, Z.; Zhang, Y.; Liu, S.; Zhang, T.Sens. Actuator B-Chem. 2016, 222, 893-903.

16. Jeevan, P.; Ramya, K.; Edith, R. Indian journal of Biotech, 2012, 11, 72.

17. Satheeskumar, S.; Ramesh, K.; Srinivasan, International Journal of Chem Tech Research,2015,7, 2478.

18. Le, N. M.; Lee, B. T. Ceramics. Int. 2016, 42, 5258-5262.

19. Dong, Y.; Zhang, X.; Cheng, X.; Xu, Y.; Gao, S.; Zhao, H.; Huo, L. .RSC Adv. 2014, 4, 57493.

20. He, Y.; Xu, B.; Li, W.; Yu, H, Agric. Food Chem. 2015, 63, 2930–2934.

21. Venkatasubramanian, K.; Sundaraj, S.Chem Sci Rev Lett., 2014, 3, 40.

22. Raj, A.; Palanisamy, K.; Arthanareeswari. M.Che. Sci. Rev. Lett., 2013, 2, 293.

